Extrapolation of rotating sound fields

Michael Carley[1]

Department of Mechanical Engineering, University of Bath, Claverton Down, Bath, BA2 7AY, United Kingdom[a)]

A method is presented for the computation of the acoustic field around a tonal circular source, such as a rotor or propeller, based on an exact formulation which is valid in the near and far fields. The only input data required are the pressure field sampled on a cylindrical surface surrounding the source, with no requirement for acoustic velocity or pressure gradient information. The formulation is approximated with exponentially small errors and appears to require input data at a theoretically minimal number of points. The approach is tested numerically, with and without added noise, and demonstrates excellent performance, especially when compared to extrapolation using a far-field assumption.

[a)] m.j.carley@bath.ac.uk

I. INTRODUCTION

The problem addressed in this paper is how to compute the acoustic field around a circular source from a limited number of measurements of the field near the source. The source in question is a disk, as a model of rotors or other tonal circular sources, and we assume that we may measure the acoustic field near the source and wish to compute it over a large range, from the near to the far field. For definiteness, we assume two possible applications. The first is the use of wind-tunnel measurements of sound near a propeller to estimate the radiated field; the second is the extrapolation of data computed on a control surface to the whole acoustic field.

In the first case, the use of wind tunnel data to estimate radiated sound, there are constraints on the data which may be acquired, arising from the difficulties and costs of experimental measurements. Especially for propellers in high speed flows, there is a strong incentive to use the smallest diameter wind tunnel possible, so that noise can only be measured in the near field of the rotor, and, for cost reasons, to measure noise at the smallest number of points consistent with accurately capturing the acoustic field. In any case, background noise in the tunnel can limit the axial range over which reliable data may be acquired. The question is then how to use these limited data to estimate noise at other points in the acoustic field.

This is not a simple task. The simplest approach is to assume an inverse distance decay of the sound amplitude, as occurs in the far field, and extrapolate measured data by scaling with distance. For this method to be valid, however, the measured data must themselves be

in the far field, defeating the purpose of the approach. Brouwer[1] presents an example using experimental data where an assumption of inverse distance decay leads to an error of 9dB in the far field level, instead of the 1dB accuracy achieved using the approach of his paper, which forms part of the method which we describe here.

There are more sophisticated techniques, such as a "transfer function" method used to project near-field data into the far field[2]. This method is used to correct noise predictions based on far-field models for near field effects and "to derive community noise levels from wind-tunnel test data". The method does, however, depend on a knowledge of the source mechanisms at work and the operating parameters of the propeller, so its generality is limited.

Another approach, which can also be applied to computed data, is based on the properties of the acoustic field, and does not require information about the source mechanisms. For example, surface integral methods[3] such as the Kirchhoff integral allow the computation of an acoustic field given only acoustic field data on a surface containing the source region. A difficulty with this approach, especially in experimental applications, is that it requires knowledge of both the acoustic pressure and velocity distribution on the bounding surface and, for accurate evaluation of the surface integral, the distribution must be resolved on a sub-wavelength scale. Even if computational rather than experimental data are being used, this can still require considerable resources.

A recent method which uses the radiation properties[4] employs a spherical harmonic expansion fitted to field data at suitably chosen points around the source, in this case a rotor. The approach does not need knowledge of source mechanisms, and requires only that the field

be captured in sufficient detail for the computation of coefficients in the spherical harmonic expansion. Given a means of computing the acoustic field, the expansion can be generated efficiently and provides a means of computing the far field for relatively low computational effort, though it still relies on being able to gather input data in the acoustic far field.

In this paper, we solve a model problem for the evaluation of the tonal acoustic field from a circular source at any point outside a cylindrical surface enclosing the source. The method as presented is exact and the approximations used to make it numerically tractable introduce exponentially small errors so that error is controlled by noise in the input data and/or field sampling limitations. The number of measurement points required appears to be the minimum theoretically possible and is very much less than the number required to avoid spatial aliasing. Unlike surface integral methods, the technique does not require acoustic velocity or pressure gradient data, and can thus be applied using standard microphone measurements or the most basic computations. Unlike existing methods, it does not require a far-field assumption and retains full accuracy over the entire acoustic field.

II. ANALYSIS

The problem to be solved is that shown in Fig. 1. A disk-shaped source of unit radius radiates into stationary fluid. A coordinate transformation is available which converts a problem with uniform mean flow into an equivalent problem with no flow[5], so this implies no loss of generality.

Given a set of measurements on a sideline, a line parallel to the axis of the source, or equivalently on a cylindrical control surface, we wish to determine the radiated field at

points outside the sideline. We adopt cylindrical coordinates (r, θ, z) with the source lying in the plane $z = 0$, and assume time dependence $\exp[-\mathrm{j}\omega t]$ with c speed of sound and free-space wavenumber $k = \omega/c$. The source is composed of a monopole and axial dipole term, "thickness" and "loading" in the propeller noise jargon, and has azimuthal order n, so that the monopole source term is of the form $s_n(r_1)\exp[\mathrm{j}n\theta_1]$ and the resulting field is $p = p_n^{(M)}\exp[\mathrm{j}n\theta]$ with

$$p_n^{(M)}(k, r, z) = \int_0^1 s_n(r_1) \int_0^{2\pi} \frac{\mathrm{e}^{\mathrm{j}(kR - n\theta_1)}}{4\pi R}\, \mathrm{d}\theta_1\, r_1\, \mathrm{d}r_1, \tag{1}$$

$$R^2 = r^2 + r_1^2 - 2rr_1\cos\theta_1 + z^2,$$

where subscript 1 denotes a variable of integration. The axial dipole term, corresponding to propeller thrust T_n,

$$p_n^{(T)}(k, r, z) = \frac{\partial p_n^{(M)}}{\partial z} = z\int_0^1 T_n(r_1) \int_0^{2\pi} \frac{\mathrm{e}^{\mathrm{j}(kR - n\theta_1)}}{4\pi R^3}\,(\mathrm{j}kR - 1)\, \mathrm{d}\theta_1\, r_1\, \mathrm{d}r_1. \tag{2}$$

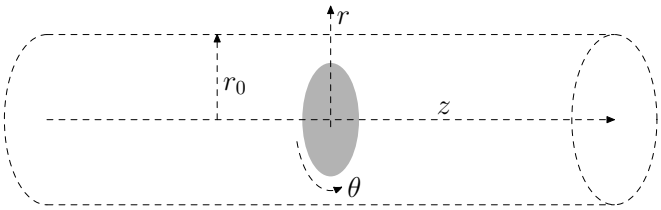

FIG. 1. Notation and coordinates for model problem.

In experimental testing, a suitable arrangement of microphones can be used to decompose a measured acoustic field into its azimuthal modes at some radius, for example by traversing an array of microphones parallel to the rotor axis. Likewise, if the objective is to extrapolate a numerically computed field, the azimuthal modes are readily computed. In any case, we

assume that we may take

$$p_n(k,r,z) = p_n^{(M)}(k,r,z) + p_n^{(T)}(k,r,z) \tag{3}$$

as the input to our method. The starting point for our technique is then $p_n(k,r,z)$ at some radial position r_0 and a set of axial stations z_i, with the location of these stations to be determined.

A. Projection of rotor noise field

There exists an exact formulation[1] for the evaluation of an acoustic field given only $p_n(k,r_0,z)$ and which, unlike a Kirchhoff method, does not require the normal derivative of acoustic pressure, but only the pressure proper, easing the evaluation of input data. The field is given by a Fourier transform of $p_n(k,r_0,z)$ followed by an inverse transform incorporating a weighting function,

$$p_n(k,r,z) = \frac{1}{2\pi}\int_{-\infty}^{\infty} \mathrm{e}^{\mathrm{j}\alpha z}\frac{H_n^{(2)}(\gamma r)}{H_n^{(2)}(\gamma r_0)}\int_{-\infty}^{\infty}\mathrm{e}^{-\mathrm{j}\alpha\xi}p_n(k,r_0,\xi)\,\mathrm{d}\xi\,\mathrm{d}\alpha, \tag{4}$$

$$\gamma^2 = k^2 - \alpha^2.$$

Here, $H_n^{(2)}(\,\cdot\,)$ is a Hankel function of the second kind, α is axial wavenumber, and ξ is the axial coordinate in the Fourier transform of $p_n(k,r_0,z)$.

Thus, given $p_n(k,r_0,z)$, $p_n(k,r,z)$ may be computed for any $r > r_0$. The difficulty lies in determining $p_n(k,r_0,z)$ with sufficient resolution to avoid spatial aliasing, and over a large enough axial range to accurately estimate the inner Fourier integral, a question addressed in Sec. II B.

For numerical evaluation, we write

$$p_n(k,r,z) \approx \frac{1}{2\pi}\int_{-k}^{k} \mathrm{e}^{\mathrm{j}\alpha z}\frac{H_n^{(2)}(\gamma r)}{H_n^{(2)}(\gamma r_0)}\int_{-Z}^{Z}\mathrm{e}^{-\mathrm{j}\alpha\xi}p_n(k,r_0,\xi)\,\mathrm{d}\xi\,\mathrm{d}\alpha, \tag{5}$$

where the axial limits $\pm Z$ are chosen so that $|p_n(\pm Z)|$ is negligible, and the infinite limits on γ are replaced by $\pm k$, the region where γ is real. Terms with γ imaginary correspond to evanescent waves[1] which decay exponentially with r and so can be neglected with negligible loss of accuracy.

In principle, we could measure $p_n(k,r_0,z)$ at a finely spaced set of points on a sideline of sufficient length to allow interpolation of the integrand and evaluation of the inner integral in Eq. 5, but in a real wind tunnel this will be made difficult by background noise limiting the axial extent over which the acoustic signal can be accurately measured and by the cost and signal drift problems in taking a number of measurements large enough for accurate interpolation. Even if the input data are generated numerically, the computational time required to generate them may rule out the use of an interpolation method. In the next section, we propose a technique for the accurate generation of $p_n(k,r_0,z)$ using an approach based on the known properties of sound from rotating sources.

B. Evaluation of acoustic field on a sideline

We now consider how to efficiently evaluate the acoustic field on a sideline. The requirement is to use a relatively small number of measurements to generate an accurate, properly-resolved, distribution of p_n over a large enough axial range for input to Eq. 5. This is made feasible by returning to some established properties of rotating sound fields. It is

known[6,7] that the acoustic field from the monopole source term is given by

$$p_n^{(M)}(k,r,z) = \sum_{m=0}^{\infty} u_{nm}(r) I_m(k,r,z), \tag{6}$$

where

$$I_m = \int_{-1}^{1} \frac{\mathrm{e}^{\mathrm{j}kR}}{R} U_m(s)(r+s)(1-s^2)^{1/2}\,\mathrm{d}s, \tag{7}$$

$$R^2 = (r+s)^2 + z^2,$$

and $U_m(s)$ is the Chebyshev polynomial of the second kind. The coefficients u_{nm} can be computed from the source distribution on the unit disk[7,8] but in this problem we do not require details of the source proper and need only the coefficients which are determined directly from field data. The function I_m can be efficiently evaluated using Gaussian quadratures based on Chebyshev polynomials of the second kind.

We now employ some properties of I_m to reduce the summation of Eq. 6 to a numerically tractable form. It is known[6] that I_m is exponentially small for $k < m+1$, so the series may be truncated with negligible loss of accuracy:

$$p_n^{(M)}(k,r,z) \approx \sum_{m=0}^{M} u_{nm}(r) I_m(k,r,z), \tag{8}$$

where the limit M depends on k. In our calculations, we take M equal to the next integer greater than k. For the thrust dipole the equivalent equation for the acoustic field is

$$p_n^{(T)}(k,r,z) \approx \sum_{m=0}^{M} v_{nm}(r) K_m(k,r,z), \tag{9a}$$

$$K_m(k,r,z) = \frac{\partial I_m}{\partial z} = z \int_{-1}^{1} \frac{\mathrm{e}^{\mathrm{j}kR}}{R^3} (\mathrm{j}kR - 1)\, U_m(s)(r+s)(1-s^2)^{1/2}\,\mathrm{d}s. \tag{9b}$$

Further source terms, such as the quadrupole which arises in high speed rotor acoustics, can be included in the method by further differentiation of I_m, at the expense of requiring a greater number of field measurements.

The total acoustic field on a sideline $r = r_0$ is then given by

$$p_n(k, r_0, z) \approx \sum_{m=0}^{M} \left[u_{nm}(r_0) I_m(k, r_0, z) + v_{nm}(r_0) K_m(k, r_0, z) \right], \tag{10}$$

and if the coefficients u_{nm} and v_{nm} can be found, $p_n(k, r_0, z)$ can be evaluated at any value of z, allowing the generation of the input to Eq. 5.

To evaluate the field at any point with $r > r_0$, Eq. 5 can be applied using the trapezoidal rule to evaluate the Fourier integrals. For evaluation of the field at a large number of points, the Fast Fourier Transform would be appropriate but the trapezoidal rule has proven adequate in the calculations presented here.

C. Summary of method

The proposed algorithm may now be summarized as follows. In a first stage,

1. for a given r_0, n, and k, select measurement points z_i and evaluate or measure $p_n^{(i)} = p_n(k, r_0, z_i)$;

2. generate the (possibly over-determined) system for Eq. 10,

$$[\mathbf{A}]\mathbf{u} = \mathbf{p},$$

   where $\mathbf{p}$ is the vector of $p_n^{(i)}$, and $\mathbf{u}$ contains the coefficients u_{nm} and v_{nm};

3. solve this system for $\mathbf{u}$;

4. use the coefficient vector $\mathbf{u}$ in Eq. 10 to evaluate $p_n(k, r_0, z)$, $-Z \leq z \leq Z$ for input to Eq. 5.

In selecting evaluation points z_i for the generation of Eq. 10, an obvious question is whether there are measurement points which are optimal for the problem.

Stationary phase analysis[6] of I_m in the limit of large k shows that in a region $-z_m < z < z_m$, $I_m(k, r, z)$ is proportional to $k^{-1/2}$ while outside this region it decays as k^{-1}. For a given radius r_0, z_m is given by

$$z_m = (\beta'^2 - C_m^2)^{1/2}(r_0 + C_m)/\beta, \tag{11a}$$

$$C_m = -r_0/4 + (r_0^2 + 8\beta'^2)^{1/2}/4, \tag{11b}$$

where $\beta = m/k$ and $\beta' = (1 - \beta^2)^{1/2}$. We hypothesize, though we cannot prove, that the optimal spacing of measurement points on the sideline will make use of this property of the function I_m. An informal motivation for this approach can be derived by assuming that in the limit of large k, $I_m(k, r, z) \approx 0$ for $|z| > z_m$. If, for example, we take $M + 1$ evaluation points at positions $(z_m + z_{m+1})/2$, the summation of Eq. 10 is approximately

$$p_n(k, r_0, z'_q) \approx \sum_{m=0}^{M-q} \left[u_{nm}(r_0) I_m(k, r_0, z'_q) + v_{nm}(r_0) K_m(k, r_0, z'_q)\right], \tag{12}$$

$$z'_q = (z_q + z_{q+1})/2,$$

with $q = 0, 1, \ldots, M$. This has the effect of making the matrix $[\mathbf{A}]$ "nearly" triangular, which we hypothesize minimizes its condition number for a given number of field evaluation points.

In practice, we select more than one evaluation point per interval, evenly spaced between successive values of z_m. For n_z points per interval, the evaluation points in each interval are

$$z_i = z_m + \frac{z_{m+1} - z_m}{n_z + 1} i, \quad i = 1, \ldots, n_z,$$

and in order to capture the dipole field, evaluation points $\pm z_i$ are used.

III. RESULTS

In order to demonstrate and test the method, we present results for two cases. The acoustic field is generated by a combination of a monopole and a dipole ring source of radius $r_1 = 1$,

$$\begin{aligned} p_n(k, r, z) = m \int_0^{2\pi} \frac{\mathrm{e}^{\mathrm{j}(kR - n\theta_1)}}{4\pi R} \, \mathrm{d}\theta_1 \\ + dz \int_0^{2\pi} \frac{\mathrm{e}^{\mathrm{j}(kR - n\theta_1)}}{4\pi R^3} \left(\mathrm{j}kR - 1\right) \, \mathrm{d}\theta_1, \end{aligned} \tag{13}$$

$$R^2 = r^2 + 1 - 2r\cos\theta_1 + z^2,$$

with source amplitudes set arbitrarily to $m = 1.5$ and $d = 1.7$, which is sufficient to introduce noticeable asymmetry into the field. To examine representative cases, we set $k = nM_t$ where M_t is interpreted as a "tip Mach number" for a rotating source or as the "mode Mach number" k/n in duct acoustics[9]. For an isolated rotor, M_t is the Mach number based on rotation speed of the source and is typically less than one. In the case where there is rotor-stator interaction, or interaction of blade rows of a counter-rotating propeller, there will be azimuthal modes with $M_t > 1$ and these will radiate efficiently. Two cases are presented, one subsonic with $n = 11$ and $M_t = 0.5$, and one supersonic with $n = 5$ and $M_t = 1.1$. In

both cases, $k = 5.5$ allowing a comparison of the behavior of the method holding k fixed and varying other relevant parameters.

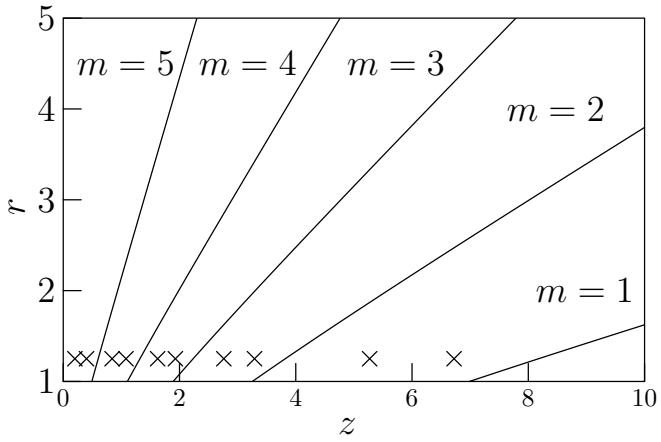

FIG. 2. Sideline evaluation points (crosses) for $n = 5$, $k = 5.5$, $r_0 = 1.25$; solid lines, transition between $k^{-1/2}$ and k^{-1} decay, from Eq. 11

Fig. 2 shows the evaluation points for $p_n(k, r_0, z)$ with $r_0 = 1.25$, with two points in each interval, $n_z = 2$. The summation of Eq. 10 is truncated at $M = 6$, the next integer greater than k and the total number of evaluation points is 20, making $[\mathbf{A}]$ a 20×14 matrix, a moderately over-determined system. Increasing the number of evaluation points beyond this number does not give large reductions in error, and so the system has been maintained at this size for the calculations presented below.

In both cases, the extrapolated field is computed at $r = 2$, $-8 \leq z \leq 8$ for the near field, and $r = 8$, $-16 \leq z \leq 16$ for the far field. In Eq. 5 the axial limit $Z = 16$ and the axial integral is evaluated using a 2048 point trapezoidal rule. For comparison, if the integrand in Eq. 5 were to be evaluated by interpolating $p_n(k, r_0, z)$ over the same axial range, a minimum of 56 points would be needed simply to sample at a half-wavelength resolution as dictated by

spatial aliasing considerations. In practice, a much larger number of points would be needed for accurate interpolation, making any such approach infeasible. From previous work[6], it appears that the method presented here requires the smallest number of measurement points for an accurate reconstruction of $p_n(k, r_0, z)$.

Comparisons of exact and extrapolated fields are plotted as real and imaginary parts, to check for phase errors, and an overall error is given as

$$\epsilon = \frac{\max |p_n^{(e)}(z) - p_n(z)|}{\max |p_n(z)|}, \tag{14}$$

where $p_n^{(e)}(z)$ is the extrapolated value on the sideline, and $p_n(z)$ is evaluated using equation 13.

Finally, for selected cases, the result of the procedure is compared to naive extrapolation assuming a simple $1/R$ decay, with the extrapolated field given by

$$p_n^{(s)}(k, r, z) = \frac{R_0}{R_s} p_n(k, r_0, z r_0/r), \tag{15}$$

$$R_0^2 = r_0^2 + (z r_0/r)^2, \quad R_s^2 = r^2 + z^2.$$

A. Noise-free data

To begin, we present graphical results for the method applied to noise-free data. The first results are those for a supersonic rotor with $M_t = 1.1$ and $n = 5$. Fig. 3 showing results for the near-field, $r = 2$, demonstrates the effectiveness of the technique, especially when compared to naive extrapolation, indicated by the crosses on the plot. Clearly, the assumption of $1/R$ decay leads to large errors and completely fails to capture even the qualitative behavior of the field.

Fig. 4 for the far field leads to similar conclusions: the field is accurately reproduced using the method of this paper, but $1/R$ extrapolation proves completely inadequate, even in a qualitative sense.

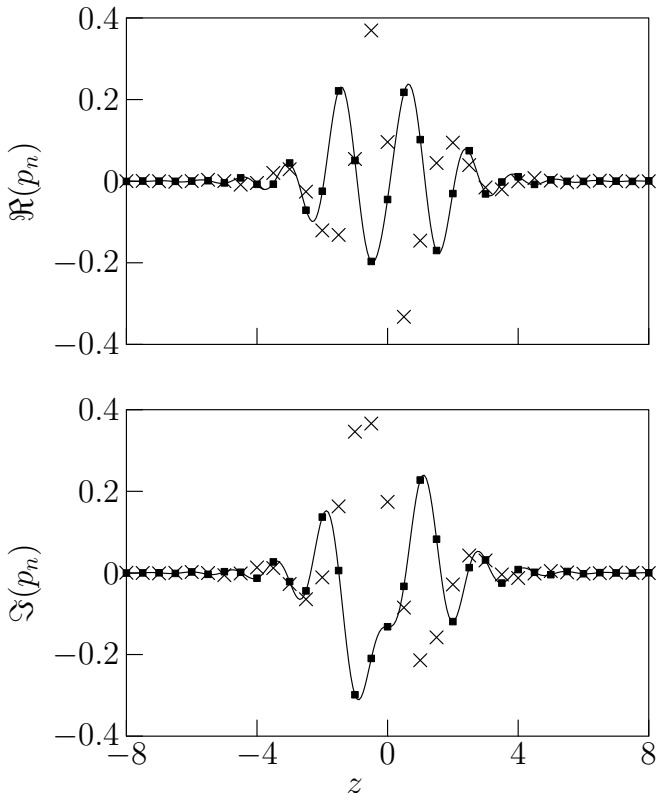

FIG. 3. Extrapolated and computed pressure on sideline $r = 2$, $n = 5$, $M_t = 1.1$: solid curve computed, boxes extrapolated, crosses $1/R$ extrapolation.

Figs. 5 and 6 show equivalent data for the subsonic case, $n = 11$, $M_t = 0.5$. Results are not presented for $1/R$ extrapolation as the errors are too large for the data to fit on the plots, as will be discussed in the next section. The quality of the extrapolation is still very good, though with a larger error in the near-field case near $z = 0$. The far field match is excellent, however, and the full variation in amplitude and phase is accurately reproduced.

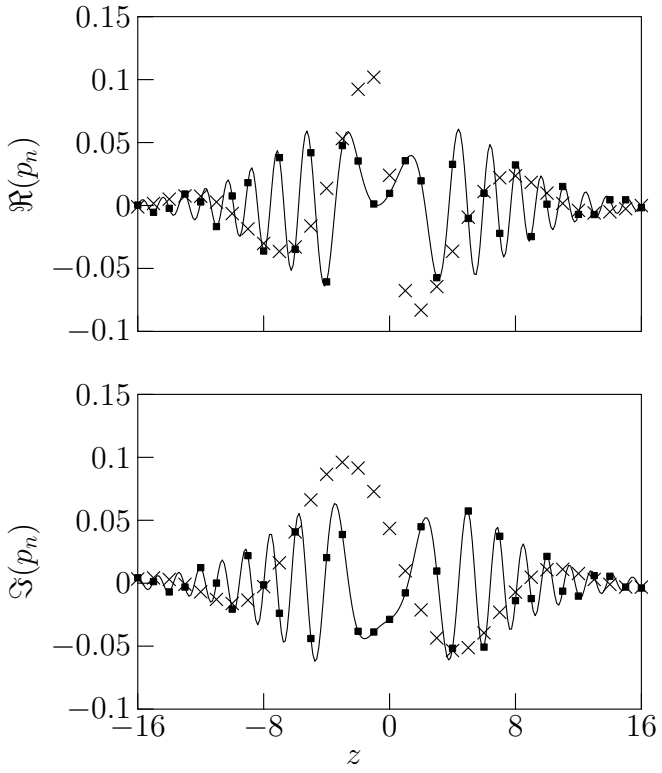

FIG. 4. Extrapolated and computed pressure on sideline $r = 8$, $n = 5$, $M_t = 1.1$: solid curve computed, boxes extrapolated, crosses $1/R$ extrapolation.

It appears that the larger error in the near field is caused by the evanescent waves which have not decayed completely by $r = 2$.

B. Effects of noise

To examine the effect of input data errors on the performance of the method, the calculations of the previous section are repeated with random fluctuations added, so that the input data are now

$$\tilde{p}_n(k, r_0, z_i) = p_n(k, r_0, z_i) + \frac{\sigma}{2^{1/2}} \frac{g_r(z_i) + \mathrm{j} g_i(z_i)}{|p_n(k, r_0, 0)|} \tag{16}$$

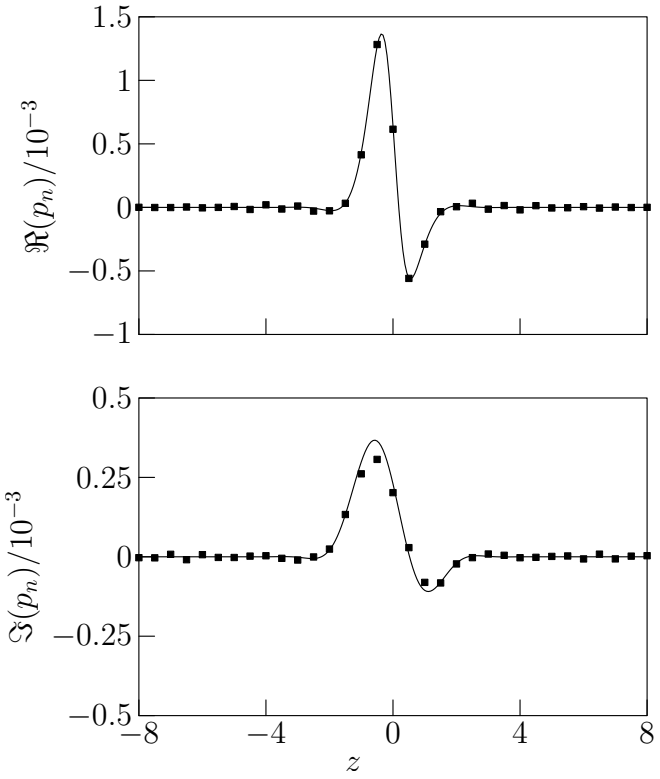

FIG. 5. Extrapolated and computed pressure on sideline $r = 2$, $n = 11$, $M_t = 0.5$: solid curve computed, boxes extrapolated.

where g_r and g_i are uniformly distributed random numbers $0 \leq g_r, g_i < 1$ and varying σ has the effect of modifying the signal-to-noise ratio based on the amplitude of the field at $z = 0$. Errors ϵ_n and ϵ_f for the near- and far-field extrapolations respectively are given in decibels, $20 \log_{10} \epsilon$, as a function of σ for the proposed method and for $1/R$ extrapolation.

Table I gives the data for the $n = 5$, $M_t = 1.1$ case and demonstrates the very good performance of the method. The first case, that with no added noise, establishes that the near-field error is less than -41dB, and the far-field less than -54dB. These errors are roughly constant until the signal-to-noise ratio reaches 40dB, when the performance of the method begins to suffer. In all cases, however, it is far superior to simple $1/R$ extrapolation,

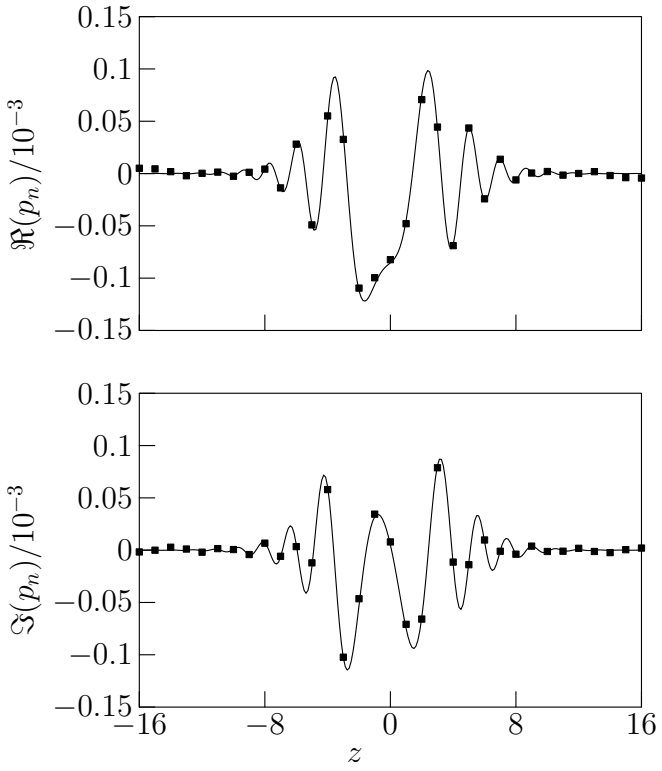

FIG. 6. Extrapolated and computed pressure on sideline $r = 8$, $n = 11$, $M_t = 0.5$: solid curve computed, boxes extrapolated.

as is shown by the final two columns of the table, and by the plotted values in Figs. 3 and 4, with the $1/R$ method over-predicting by about 9dB in the worst case, similar to the error noted by Brouwer[1] for a different case using experimental data.

Table II shows equivalent data for the subsonic case. As was apparent from the plotted results, the error in this case is larger than for $M_t = 1.1$, although this should be compared to the very much larger error for $1/R$ extrapolation, which is more than 40dB in the far field.

TABLE I. Error in near- and far-field extrapolations for $n = 5$, $M_t = 1.1$ with added noise

	Extrapolation		$1/R$ extrapolation	
$20\log_{10}\sigma$	$20\log_{10}\epsilon_n$	$20\log_{10}\epsilon_f$	$20\log_{10}\epsilon_n$	$20\log_{10}\epsilon_f$
—	-41.5	-54.5	8.5	7.4
-80.0	-41.5	-54.7	8.5	7.4
-60.0	-41.6	-53.5	8.5	7.4
-40.0	-38.7	-41.6	8.5	7.4
-20.0	-20.5	-17.5	8.6	7.5

C. Distribution of measurement points

To illustrate the effect of the sampling point distribution on the quality of results, we repeat the calculation with $n = 10$, $M_t = 1.1$, $k = 11$, comparing the results using sampling points found using Eq. 11 and a linear distribution. For the standard sampling, we use two points per interval, as in the previous section, giving a total of forty sampling points with $-14 < z_i < 14$. For the linear sampling, we use forty equally spaced points with $-3.5 < z_i < 3.5$. The interval was shortened because in the added-noise cases, the data over much of the interval would otherwise be swamped with noise. Linear spacing over the range $-7 < z_i < 7$ gave similar results, though with larger error in the higher noise cases. For comparison, if the field were to be sampled at four points per wavelength, for

TABLE II. Error in near- and far-field extrapolations for $n = 11$, $M_t = 0.5$ with added noise

	Extrapolation		$1/R$ extrapolation	
$20\log_{10}\sigma$	$20\log_{10}\epsilon_n$	$20\log_{10}\epsilon_f$	$20\log_{10}\epsilon_n$	$20\log_{10}\epsilon_f$
—	-26.9	-24.8	27.4	42.3
-80.0	-26.9	-24.8	27.4	42.3
-60.0	-26.9	-25.2	27.4	42.3
-40.0	-27.0	-24.9	27.4	42.3
-20.0	-19.9	-14.7	27.6	42.2

direct interpolation, one hundred sample points would be required to cover the interval $-7 < z_i < 7$.

The condition number of the matrix $[\mathbf{A}]$ for the standard and linear sampling is 2×10^7 and 2×10^8 respectively, an order of magnitude difference, though neither matrix poses a difficulty for a standard linear solver. Table III, however, shows very different behavior with respect to added noise. For the smaller amounts of added noise, the near-field error is comparable in the two cases, though there is a large difference in far-field error even for the noise-free case. At the 40dB signal-to-noise ratio, the near-field error for standard spacing is worse than for the linear case, but the far-field result is much better. For the highest added-noise case, neither approach gives accurate results for this configuration, but the far-field error for the linear spacing is especially large. It appears that the sample point spacing has

TABLE III. Error in near- and far-field extrapolations for $n = 10$, $M_t = 1.1$ for linear and non-linear sample point spacing

	Eq. 11 spacing		Linear spacing	
σ/dB	ϵ_n/dB	ϵ_f/dB	ϵ_n/dB	ϵ_f/dB
—	-65.9	-73.4	-63.3	-45.2
-80.0	-59.8	-63.3	-54.8	-36.5
-60.0	-48.0	-48.7	-37.0	-18.7
-40.0	-9.3	-12.2	-15.7	2.6
-20.0	9.4	6.6	8.7	26.6

little effect on the computed near field, but that the result for the far field is much better when sample points are chosen based on Eq. 11, lending weight to the hypothesis that this may be the optimal sampling strategy.

IV. CONCLUSIONS

We have presented a technique for the extrapolation of rotating sound fields based on field measurements on a cylindrical surface surrounding an arbitrary tonal source. The approach can be used with experimental data, such as those taken in wind-tunnel testing of propellers, or with numerically-computed input, making it an attractive alternative to the Kirchhoff method in some applications. Numerical testing, including the effect of noise,

has demonstrated that the method is efficient, requiring far fewer input data than would be needed to avoid spatial aliasing, and that it is accurate even in the presence of added noise. We hypothesize, though we have not proved, that the method for selection of field sample points is optimal, and preliminary results on the condition number of the method seem to lend weight to this view. Overall, the method is based on a formulation with exponentially small errors, and is easily implemented using standard tools, making it an attractive means of computing noise fields given limited data.

REFERENCES

[1]H. H. Brouwer, "Analytic description of the noise radiation from single- and counter-rotating propellers," NLR-TP-2011-295, Nationaal Lucht- en Ruimtevaartlaboratorium (2011).

[2]N. Peake and W. K. Boyd, "Approximate method for the prediction of propeller noise near-field effects," Journal of Aircraft **30**(5), 603–610 (1993).

[3]A. S. Lyrintzis, "Surface integral methods in computational aeroacoustics—From the (CFD) near-field to the (Acoustic) far-field," International Journal of Aeroacoustics **2**(2), 95–128 (2003) doi: 10.1260/147547203322775498.

[4]Y. Mao and C. Xu, "Accelerated method for predicting acoustic far field and acoustic power of rotating source," AIAA Journal **54**(2), 603–615 (2016) doi: 10.2514/1.J054425.

[5]C. J. Chapman, "Similarity variables for sound radiation in a uniform flow," Journal of Sound and Vibration **233**(1), 157–164 (2000).

[6]M. Carley, "Analysis of the radiated information in spinning sound fields," Journal of the Acoustical Society of America **128**(4), 1679–1684 (2010) doi: 10.1121/1.3478852.

[7]M. Carley, "The radiating part of circular sources," Journal of the Acoustical Society of America **129**(2), 633–641 (2011) doi: 10.1121/1.3531925.

[8]M. J. Carley and P. A. Martin, "Jet noise: sound generation by disc and cylinder sources," Proceedings of the Royal Society of London. A. **468**(2148), 3947–3964 (2012) doi: 10.1098/rspa.2012.0362.

[9]J. M. Tyler and T. G. Sofrin, "Axial flow compressor noise studies," Transactions of the Society of Automotive Engineers **70**, 309–332 (1962).